

HLSTester: Efficient Testing of Behavioral Discrepancies with LLMs for High-Level Synthesis

Kangwei Xu¹, Bing Li², Grace Li Zhang³, Ulf Schlichtmann¹

¹Chair of Electronic Design Automation, Technical University of Munich, Munich, Germany

²Research Group of Digital Integrated Systems, University of Siegen, Siegen, Germany

³Hardware for Artificial Intelligence Group, Technical University of Darmstadt, Darmstadt, Germany

kangwei.xu@tum.de, bing.li@uni-siegen.de, grace.zhang@tu-darmstadt.de, ulf.schlichtmann@tum.de

ABSTRACT

In high-level synthesis (HLS), C/C++ programs with synthesis directives are used to generate circuits for FPGA implementations. However, hardware-specific and platform-dependent characteristics in these implementations can introduce behavioral discrepancies between the original C/C++ programs and the circuits after high-level synthesis. Existing methods for testing behavioral discrepancies in HLS are still immature, and the testing workflow requires significant human efforts. To address this challenge, we propose **HLSTester**, a large language model (LLM) aided testing framework that efficiently detects behavioral discrepancies in HLS. To mitigate hallucinations in LLMs and enhance prompt quality, the testbenches for original C/C++ programs are leveraged to guide LLMs in generating HLS-compatible testbenches, effectively eliminating certain traditional C/C++ constructs that are incompatible with HLS tools. Key variables are pinpointed through a backward slicing technique in both C/C++ and HLS programs to monitor their runtime spectra, enabling an in-depth analysis of the discrepancy symptoms. To reduce test time, a testing input generation mechanism is introduced to integrate dynamic mutation with insights from an LLM-based progressive reasoning chain. In addition, repetitive hardware testing is skipped by a redundancy-aware filtering technique for the generated test inputs. Experimental results demonstrate that the proposed LLM-aided testing framework significantly accelerates the testing workflow while achieving higher testbench simulation pass rates compared with the traditional method and the direct use of LLMs on the same HLS programs.

1 INTRODUCTION

As the demand for hardware performance in AI computing continues to grow, an increasing number of software applications originally designed for CPUs are being ported to specialized hardware accelerators like FPGAs [1–4]. High-Level Synthesis (HLS) tools can take general-purpose programming languages such as C/C++ and generate Hardware Description Languages (HDL), thereby synthesizing corresponding circuits for FPGA deployment [5, 6].

Due to limitations of HLS tools, only a subset of C/C++ programs is supported, referred to as HLS programs [7]. When these programs are synthesized into circuits by the HLS tool, they may exhibit behavioral discrepancies compared to the original C/C++ programs running on CPUs. Such discrepancies include overflow or truncation from customized bit width, out-of-bounds memory accesses caused by static allocation, and data dependencies due to pipelining, etc. For example, default data types in CPU instructions are typically represented as *int* or *float*, whereas in FPGA designs, the bit width of integers and floats are often customized, which could lead to overflows on FPGAs. Additionally, FPGAs enable

parallel computing through pipeline execution by incorporating *hardware directives* such as `#pragma HLS pipeline`, which may produce results that differ from those of sequential CPU execution, particularly in cases where data dependencies or feedback paths exist among functions. Therefore, testing behavioral discrepancies is important, as programs that execute correctly on CPUs may still fail or produce incorrect results when deployed on FPGAs [10–12].

To test behavioral discrepancies in HLS, developers typically need to monitor runtime spectra (e.g., the dynamic traces of variable values, accessed offsets, and stack/FIFO queue sizes) by constructing testbenches and instrumenting key variables. Any discrepancies in these spectra between C/C++ programs on CPUs and synthesized circuits on FPGAs can reveal issues in HLS that need to be addressed [13, 14]. However, this process requires developers to have expertise in both hardware and software, with significant efforts in the overall testing workflow. In addition, developers generally employ fuzz testing [15], a common test input generation scheme that has been widely applied in software testing where each test input run completes in just a few milliseconds [16]. However, in hardware testing, particularly in FPGA testing where clock-cycle-level simulation is required due to data dependencies, the testing latency (i.e., the time required to perform a test operation) often ranges from several minutes to several hours, rather than milliseconds [17, 18]. Moreover, test inputs generated by fuzz testing do not take hardware platform characteristics into account, making it ineffective in testing behavioral discrepancies in HLS.

Large language models (LLMs) have shown great potential in automated software and hardware design, thereby supporting the entire process from initial concepts to design, testing, verification, and physical implementation [19–26]. Recent research has shown that LLMs can be employed to test errors in C/C++ programs and Hardware Description Language (HDL) designs. CityWalk [28] leverages project-dependency analysis and insights from documentation to address complex features, such as pointers, templates, and virtual functions, thus producing high-quality testbenches. CorrectBench [29] employs LLMs to implement a testing platform with self-correction, and an evaluation framework is proposed to evaluate the performance of the generated testbenches. VerilogReader [30] leverages LLMs to interpret Verilog code, aiming to generate code convergence tests. A testing interpreter is introduced to enrich prompts and enhance LLM’s understanding of the testing intent.

Previous methods above use LLMs to test simple errors in common code types, such as individual C/C++ or Verilog programs that LLMs are extensively trained on and thus highly familiar with. However, these methods do not provide a comprehensive testing workflow to detect discrepancy symptoms in interdisciplinary fields such as HLS, which require both hardware and software exploration. In this paper, an LLM-aided HLS testing framework, **HLSTester**, is

Table 1: Typical sources of discrepancies when porting C/C++ programs from CPU to FPGA via High-Level Synthesis.

Type	#Pragma	Description	Typical Difference
Data Type	<code>typedef ap_uint<x> bitx</code>	Unsigned int	Overflow & truncation can cause discrepancies
	<code>typedef ap_int<x> bitx</code>	Signed int	
Memory	<code>#pragma HLS array_reshape</code>	Reshape array	Allocate a large array <code>int x[m][n]</code> causes errors on FPGA but not on CPU
	<code>#pragma HLS array_partition</code>	Split array	
Parallel	<code>#define size M</code>	Set static array	
	<code>#pragma HLS pipeline</code>	Concurrent op.	Feedback paths may lead to different results
Loop	<code>#pragma HLS dataflow</code>	Task pipelining	
	<code>#pragma HLS unroll</code>	Duplicate loops	Different results due to incorrect unrolling on FPGA
	<code>#pragma HLS loop_flatten</code>	Flatten loops	
Recursion	NA	NA	Exceed stack size

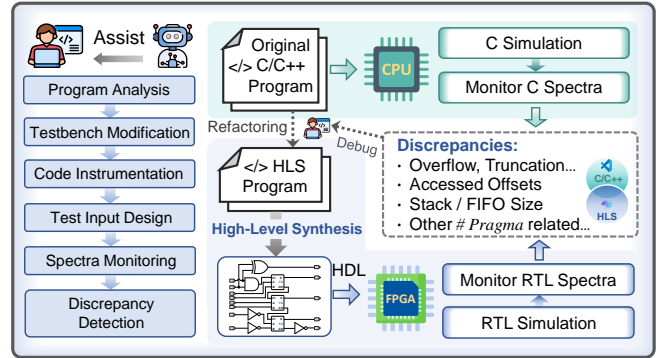
proposed that employs an iterative testing workflow to automatically detect behavioral discrepancies in the HLS design. The key contributions of this paper are summarized as follows.

- We propose an efficient testing framework for HLS that covers code analysis, testbench generation, and runtime profiling for behavioral discrepancy detection.
- By leveraging the adaptive learning capability of LLMs, existing C/C++ testbenches are used as references to guide the LLM to generate testbenches that are compatible with the HLS tool, which improves the simulation pass rate of the generated testbenches by an average of 20.67%.
- To enable an in-depth analysis of the discrepancy, a backward slicing technique, combined with the semantic understanding capabilities of LLMs, is employed to instrument the HLS program. Monitoring scripts are also developed to record the runtime spectra of key variables, which could also provide a reliable basis for subsequent test input mutation.
- A test input generation mechanism is proposed that leverages spectra feedback to guide dynamic mutation, along with insights from an LLM-based progressive reasoning chain. The LLM-guided test input generation achieves an average of $1.81\times$ speedup in detecting all behavioral discrepancies, while the dynamic mutation further increases the speedup to an average of $2.28\times$.
- To further reduce the latency of HLS testing, a redundancy-aware technique is proposed to identify and skip repetitive hardware simulations among the generated test inputs, which contributes an additional 15.73% acceleration in the testing workflow.

The rest of this paper is organized as follows. Section 2 provides the background and motivation for this work. Section 3 details the proposed framework. The experimental results are provided in Section 4. Section 5 concludes the paper.

2 BACKGROUND AND MOTIVATION

Since some traditional C/C++ constructs are not supported by HLS tools or lead to inefficient synthesized circuits, significant code refactoring and the incorporation of specific hardware directives are necessary to adapt them for synthesis and optimization [7]. Testing behavioral discrepancies between the original C/C++ programs and the circuits after high-level synthesis is challenging due to assumptions made during hardware synthesis. Table 1 presents typical examples of how directives cause these discrepancies [8].

**Figure 1: Traditional workflow for testing behavioral discrepancies in High-Level Synthesis.**

◦ *Data Type*: HLS supports arbitrary bit width for variables, leading to a reduction in FPGA resource usage. For example, analysis of the variable ‘m’ in a standard C++ program exhibits a minimum value of 0 and a maximum of 481, thereby necessitating only 9 bits instead of the 32-bit `int` type. In such cases, the directive `#typedef ap_uint<9>` is used to declare a 9-bit arbitrary precision integer. With custom bit width, FPGAs become more susceptible to overflow, potentially leading to incorrect results.

◦ *Memory Management*: HLS tools do not support dynamic arrays because FPGAs are unable to manage unbounded data structures. As a result, functions such as `malloc()` should be replaced with pre-allocated static arrays of estimated size [31]. Accessing an unexpected address may cause the FPGA to return an incorrect output.

◦ *Parallelization and Loop*: Hardware directives such as `#pragma HLS pipeline` can be inserted within loops to enable pipelining, allowing multiple input streams to be processed concurrently within the same clock cycle, thereby improving data throughput. The directive `#pragma HLS unroll` creates multiple instances of a loop body in the generated RTL design, enabling partial or complete parallel execution of loop iterations. In addition, the directive `#pragma HLS dataflow` enables task-level pipelining, allowing functions and loops to overlap their operations [32]. However, such parallel execution can produce results that differ from sequential CPU execution, particularly when misaligned data accesses occur or feedback paths exist between different variables or functions.

◦ *Recursion*: HLS tools do not support dynamic stack allocation for execution states, so recursion needs to be converted to iteration using a finite-size stack [33]. When recursion depth exceeds the pre-estimated size, FPGA compilation failures occur.

An overview of the traditional workflow for testing behavioral discrepancies in HLS is shown in Fig. 1. Typically, developers begin with a program analysis, followed by modifications to the testbench to eliminate certain traditional C/C++ constructs that are incompatible with HLS tools. Then, both the original C/C++ programs and their HLS counterparts are instrumented, and a set of relevant test inputs is designed. At runtime, key spectra values (i.e., variable traces) are recorded and compared between the original C/C++ program and the circuits after high-level synthesis, and any mismatches in these spectra indicate behavioral discrepancies.

To generate these test inputs in the HLS workflow, several methods are typically employed: (1) random generation using data generators [34]; (2) handcrafted inputs by an HLS expert; or (3) systematic

```

1: int main(int argc, char *argv[]) { (a) C++ Code
2: int accum = 0; int thres = argv[1];
3: int arr_data[];
4: for (int p = 0; p < arr_data.size(); p++) {
5:   accum += arr_data[p];
6: for (int p = 0; p < arr_data.size(); p++) {
7:   (arr_data[p] /= accum) > th ?
8:   process(argv[2]) : backup(argv[3]);}
}

1: #include "ap_int.h" (b) HLS Code
2: #include "hls_stream.h"
3: #define M 256 Static array & Customized Bit Widths
4: typedef ap_uint<8> 8bits; typedef ap_uint<11> 11bits;
5: 8bits arr_data[M], 11bits accum = 0;
6: int ac(arr_data[M], size, &accum) {
7:   for (int p = 0; p < size; p++) {Unrolled loop in HLS
8:     #pragma HLS unroll factor=2
9:     accum += arr_data[p];} return 0;}
10: void top(thres, *proc_path, *backup_path) {
11:   #pragma HLS INTERFACE HLS-Specific
12:   #pragma HLS pipeline Hardware Directives
13:   hls::stream<char> proc, backup;
14:   ac(arr_data, size, accum);
15:   for (int p = 0; p < size; p++) {
16:     #pragma HLS unroll factor=2
17:     if ((arr_data[p] /= accum) > thres) {
18:       proc << proc_path[p];
19:     } else {backup << backup_path[p];}
20: int main(int argc, char *argv[]) {
21:   int thres=argv[1]; top(thres, argv[2], argv[3]);}

```

Figure 2: Example of behavioral discrepancies between (a) the original C++ code and (b) the HLS code.

enumeration through scripts [35]. Typically, the test input generation technique begins with a set of seed inputs, selecting one seed randomly and producing new inputs by altering a few bits or bytes. However, this method relies on the assumption that the target program completes execution in milliseconds during software testing. However, in FPGA testing, a single hardware synthesis and testing simulation may take several minutes or even hours. Moreover, traditional mutation techniques in software testing overlook hardware-specific characteristics such as custom bit widths, static memory allocation, and pipelining via hardware directives, resulting in ineffective behavioral discrepancy testing in HLS.

To illustrate the need for testing behavioral discrepancies in HLS environments, Fig. 2(a) presents an edge processing task. In this task, the original C++ program first computes the cumulative sum of an image gradient vector and then compares the percentage of each gradient against a threshold to decide whether to process pixels. In Fig. 2 (b), to address the performance bottleneck on the CPU and fully exploit FPGA parallelism, the developer refactored the C++ code, which introduced custom bit width, static arrays, and various hardware directives. However, these hardware-specific refactoring may induce platform-dependent behavioral discrepancies. For example, custom bit width could result in overflow, division-by-zero, or truncation issues; replacing dynamic memory allocation with static arrays may lead to out-of-bound accesses; and the pipelining may produce results that differ from sequential CPU execution.

Therefore, it is necessary to develop an efficient testing framework tailored for HLS. Contrary to previous work, the proposed **HLSTester** leverages the in-context learning and comprehension capabilities of LLMs to assist key testing points. Integrating testing scripts with feedback from HLS tools accelerates discrepancy testing and results in a more efficient testing workflow.

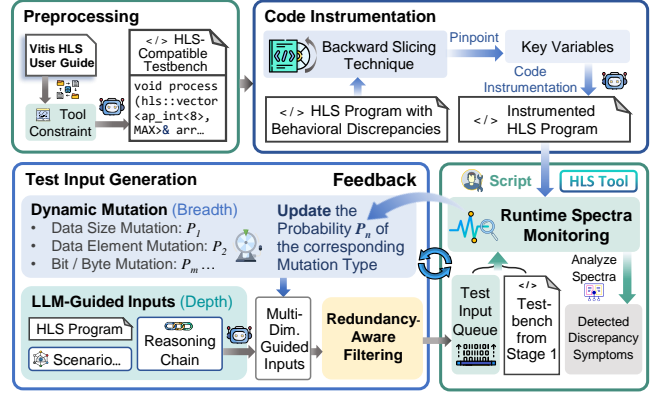


Figure 3: Testing Workflow of HLSTester.

3 LLM-AIDED BEHAVIOR DISCREPANCY TESTING FOR HIGH-LEVEL SYNTHESIS

To efficiently detect behavioral discrepancies between the original C/C++ programs and the circuits after high-level synthesis, we propose an LLM-aided testing framework composed of five stages: preprocessing, code instrumentation, spectra monitoring, test input generation, and redundant test input filtering. As illustrated in Fig. 3, the framework first constructs a testbench compatible with the HLS tool by eliminating incompatible C/C++ constructs. Next, a backward slicing technique is employed to pinpoint key variables, which are then instrumented to enable real-time monitoring of their runtime spectra. The collected spectra are fed back into the test input generation stage to guide the dynamic mutation of the test inputs, forming a cyclic feedback system. Finally, a redundancy-aware filtering mechanism for the generated test inputs is applied to skip duplicate hardware simulations. Each stage will be illustrated in detail in the following subsections.

3.1 Preprocessing

Certain C/C++ constructs in C/C++ testbenches, such as traditional C/C++ header files, definitions for dynamic arrays, and other unsupported features, are incompatible with HLS tools. However, despite the strict constraints imposed by HLS tools, both types of testbenches exhibit notable similarities in their intended functionality and basic structure. To enable the generation of a testbench compatible with HLS tools, three key components are prepared: (1) the original C/C++ program, (2) its corresponding C/C++ testbench, and (3) a refactored version of the program, referred to as the HLS program under test, which complies with the constraints of the HLS tool. At this stage, given the adaptive learning capabilities of LLMs, existing C/C++ testbenches are used as references to guide the generation of testbenches suited for HLS tools. We formalize this HLS-compatible testbench generation as follows:

$$F_{LLM} : T_{C/C++} \rightarrow T_{HLS}, \text{ s.t. Constraints}_{HLS}, \quad (1)$$

where $T_{C/C++}$ is the set of traditional C/C++ testbenches, T_{HLS} is the set of HLS-compatible testbenches, Constraints_{HLS} are the constraints imposed by HLS tools. The LLM needs to focus on the following aspects during the analysis and generation process:

(1) Code Semantic Analysis: The LLM performs a semantic analysis of the C++ testbench to understand its core logic, functionality, and structure. This step ensures that the LLM fully captures the

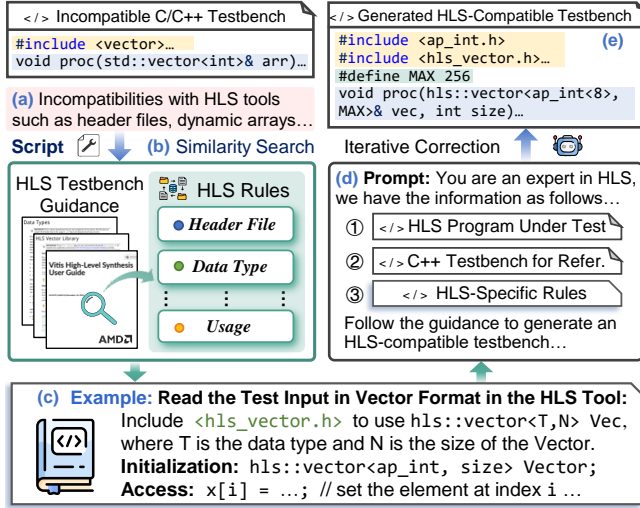


Figure 4: LLM-aided HLS-compatible testbench generation.

key functionalities and operations in generating a testbench that is compatible with the HLS tool.

(2) Usage limitations: To meet HLS tool requirements, the LLM adjusts the header files and data types in the original C/C++ testbench to match the definitions provided in the HLS User Guide. For instance, standard data transfers in C++ need to be changed to stream-based data transfers by including the `<hls_stream.h>` header file and using the `hls::stream` class to emulate hardware stream processing structures. Data types should also be adapted for the HLS program, such as replacing the default `int` type in the C++ testbench with the `ap_int` type.

To enhance the prompts of LLMs, a Retrieval-Augmented Generation (RAG) technique is employed by incorporating external expert guidance via a retriever. This process involves three stages:

① An external rule library is created containing HLS rule templates. Each template includes potential error logs that may be encountered during synthesis, a brief summary of the associated HLS rule, and usage examples extracted from the HLS tool manual.

② The existing C/C++ testbench is compiled with the HLS tool, and its error logs are used as queries to retrieve matching templates from the rule library. These rule templates embed potential error logs that not only facilitate matching with the compiler-generated error logs but also incorporate guidelines for correcting these errors. A sentence transformer [43] is used to convert the compiler-generated error log and each rule template into embedding vectors. The retrieval process can be formalized as follows:

$$E = \text{embed}(\text{error_log}), \quad R_i = \text{embed}(\text{rule_template}_i), \quad (2)$$

where E and R_i represent the embedding vectors of the compiler-generated error log and the i th rule template, respectively. Given an error log with embedding E and a rule template with embedding R , their similarity is computed using the cosine similarity, and the rule template with the highest similarity is selected as follows:

$$\text{sim}(E, R) = \frac{E \cdot R}{\|E\| \|R\|} \quad \text{and} \quad R^* = \arg \max_{R_i \in \mathcal{R}} \text{sim}(E, R_i), \quad (3)$$

where \mathcal{R} denotes the set of all rule templates in the library, R^* is the rule template from \mathcal{R} that has the highest cosine similarity with the compiler-generated error log embedding E .

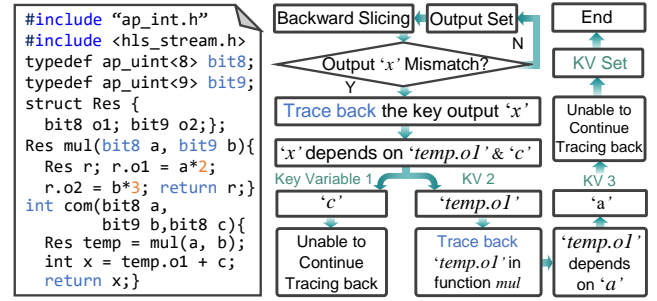


Figure 5: Using backward slicing technique to pinpoint key variables in the HLS program.

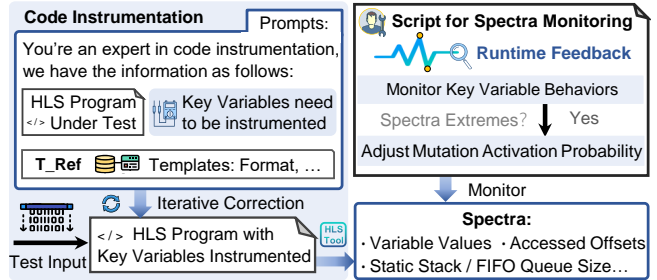


Figure 6: Code instrumentation and spectra monitoring.

③ Once the template with the highest similarity is retrieved, its content is incorporated into the prompt provided to the LLM to generate an HLS-compatible testbench.

To illustrate the application of RAG in generating an HLS compatible testbench, we present an example as shown in Fig. 4. Initially, when the HLS compiler detects incompatible errors (a), such as those related to the use of `<vector>` and dynamic arrays, it generates error logs. These error logs are then used to retrieve the most appropriate rule template from the external library via a sentence transformer (b). Once the rule template with the highest similarity is identified (c), for example, one that recommends replacing `<vector>` with `<hls_vector.h>`, it is incorporated into the prompt provided to the LLM (d). The LLM then follows this guideline to generate a new testbench (e). If the HLS compiler still detects an error, the process iteratively repairs the testbench until a correct version that conforms to HLS constraints is obtained.

3.2 Code Instrumentation and Runtime Spectra Monitoring for Discrepancy Analysis

To enable an in-depth analysis of discrepancies, a backward slicing technique, combined with the semantic understanding capabilities of LLMs, is employed to instrument key variables within the program, and monitoring scripts are developed to record their runtime spectra. Backward slicing is a program analysis technique that traces data dependencies in reverse from a target output to identify all variables that affect its value [40]. For example, in a function that computes an output through a series of intermediate calculations, backward slicing can identify the relevant variables that contribute to the final result. Consider a dependency graph $G = (V, E)$, where V is the set of variables and E is the set of dependency edges. Let x be the target output variable that needs to be traced back. The backward slicing process is then formalized as follows:

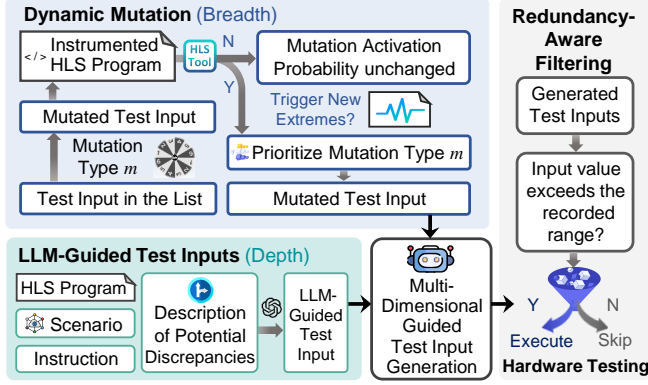


Figure 7: Test input generation and redundancy-aware filtering.

$$S_0 = \{x\}, \quad S_{i+1} = S_i \cup \{u \in V \mid \exists v \in S_i : (u, v) \in E\}, \quad (4)$$

where S_0 starts with the target output variable x , and with each iteration, any variable u that influences a variable v already in the current slice S_i is added to form the next slice S_{i+1} . The slicing process is repeated until no new variables can be added, i.e., when $S_{i+1} = S_i$, and the resulting slice is denoted by $S(x) = S_i$. The set of key variables, denoted as KV, is defined as all the variables in the backward slice except the output variable itself:

$$KV(x) = \{v \in S(x) \mid v \neq x\}, \quad (5)$$

meaning any variable that contributes (directly or indirectly) to the final output x is considered a key variable.

To illustrate the process of the backward slicing technique, a simple example is presented in Fig. 5. The process begins at the target output variable x , where discrepancies between C/C++ execution and RTL simulation are observed. Analysis shows that x depends on *temp.o1* and c . Since c cannot be traced further, it is identified as a key variable (KV). The slicing then traces *temp.o1* in the *mul* function and reveals its dependence on a , which is subsequently marked as a key variable. The final set of key variables is therefore $KV(x) = \{temp.o1, c, a\}$, and these variables are targeted for instrumentation and runtime monitoring.

To facilitate runtime monitoring, our framework leverages an LLM to instrument the program using the previously pinpointed key variables. As shown in Fig. 6, once the key variables are pinpointed, the HLS code is integrated with predefined instrumentation templates, which are provided to the LLM as prompts. These templates specify how to add instrumentation constructs and specify the output format for the runtime spectra. The LLM then generates an instrumented version of the HLS code that records the runtime spectra $Spectra(V)$ of these variables, which can be defined as follows: $Spectra(V) = \{(\text{val}(V), \text{offset}(V), \text{loop}(V), \text{stack}(V), \text{FIFO}(V))\}$, where $\text{val}(V) = [\min(V), \max(V)]$ denotes the recorded value range, $\text{offset}(V)$ captures array offsets, $\text{loop}(V)$ records loop iteration counts, $\text{stack}(V)$ represents static stack usage, and $\text{FIFO}(V)$ tracks FIFO queue sizes. The runtime spectra are subsequently analyzed by a monitoring script, which generates detailed reports to highlight discrepancy symptoms such as overflow, division by zero, and truncation. Table 1 summarizes the five categories of spectra currently supported by this framework; these mappings can be extended by modifying a configuration file. For instance, array access offsets are monitored to detect out-of-bounds behavior, and actual loop iteration counts are verified to ensure that loop unrolling

Table 2: Dynamic mutation.

Mutation ID	Type/Inputs	Key Variable Spectra			Range/Size	Mutation Activation Probability
		Type	Name	Min Max		
Seed	N/A	Input	arr_data	1 7	(1, 7)	[0.125, 0.125,
	[1,1,7,5]	Variable	accum	2 14	(2, 14)	0.125, 0.125,
		Mem_ofs	arr_data	[0, 1, 2, 3]	4	0.125, 0.125,
		Loop	Iteration	N/A 2	2	0.125, 0.125]
1	T ₂	Input	Input	1 7	(1, 7)	[0.125, 0.125,
	[1,4,2,7]	Variable	sum	2 14	(2, 14)	0.125, 0.125,
		Mem_ofs	Input	[0, 1, 2, 3]	4	0.125, 0.125,
		Loop	Iteration	N/A 2	2	0.125, 0.125]
2	T ₅	Input	Input	1 8	(1, 8)	[0.119, 0.119,
	[1,5,8,3]	Variable	sum	2 17	(2, 17)	0.119, 0.119,
		Mem_ofs	Input	[0, 1, 2, 3]	4	0.165, 0.119,
		Loop	Iteration	N/A 2	2	0.119, 0.119]
3	T ₁	Input	Input	1 9	(1, 9)	[0.159, 0.114,
	[4,2,5,9,1]	Variable	sum	2 21	(2, 21)	0.114, 0.114,
		Mem_ofs	Input	[0, 1, 2, 3, 4]	5	0.159, 0.114,
		Loop	Iteration	N/A 3	3	0.114, 0.114]

optimizations align with expectations. Furthermore, the monitoring script reports a feedback array (e.g., `spectra_feedback`) that records the type, name, minimum, and maximum value of each variable in Table 2. This feedback also provides a basis for subsequent dynamic mutation, which will be detailed in the next subsection.

3.3 Multi-Dimensional Guided Test Input Generation for Effective Testing

To achieve a comprehensive exploration of both breadth and depth in the test input space, two complementary techniques are integrated for test input generation: dynamic mutation and LLM-guided mechanism. As shown in Fig. 7, the dynamic mutation approach broadly explores the test input space by applying a diverse set of mutation operations, while the LLM-guided mechanism uses semantic analysis to generate test inputs that target unique execution paths. Through multiple rounds of validation, 30% of test inputs are generated by the LLM, focusing on program insights, while the remaining test inputs are generated via dynamic mutation to ensure broad coverage.

3.3.1 Dynamic Mutation. As different mutations vary in their ability to trigger different behaviors [41, 42], prioritizing effective mutation operations to test platform-dependent behaviors in HLS presents a significant challenge. In our framework, activation probabilities for mutation types are dynamically adjusted to prioritize those that produce new spectra values, thereby increasing the chances of revealing platform-dependent behavioral discrepancies. Since FPGA test inputs are typically arrays or matrices, our scheme employs eight mutation types to generate new test inputs:

- ① *Data Size Mutation*: Inserts or deletes random elements in the test input, e.g., changing the input $[h, i, j]$ to $[h, i, j, k]$.
- ② *Data Dimension Mutation*: Adjusts matrix dimensions, such as adding or removing a row/column, e.g., modifying $[[h, i, j], [m, n, p]]$ to $[[h, i, j], [m, n]]$ or $[[h, i], [m, n]]$.
- ③ *Zero Value Mutation*: Sets the elements to zero, e.g., changing an element in the array $[h, i, j]$ to 0 to obtain $[h, 0, j]$.
- ④ *Order Mutation*: Rearranges the order of elements, e.g., transforming the array $[h, i, j]$ to $[i, j, h]$.
- ⑤ *Data Element Mutation*: Alters the values of elements, e.g., converting $[h, i, j]$ to $[h, i, k]$.

⑥ *Data Type Mutation*: Changes the data type while keeping the same value, e.g., converting the integer 2 to the floating-point 2.0.

⑦ *Bit Mutation*: Randomly flips one or more bits.

⑧ *Byte Mutation*: Randomly flips one or more bytes.

Traditional fuzz testing typically assigns uniform activation probabilities to all mutation types, which restricts its adaptability to specialized hardware platforms. In contrast, our framework dynamically adjusts the activation probabilities in real-time according to monitored spectra feedback, prioritizing those mutations that trigger new spectra extremes.

Given $l = 8$ types of mutation operations, each is initially assigned an activation probability of $P_m^{(0)} = \frac{1}{l} = 0.125$. In each iteration t , a mutation operation T_m is selected to generate an input. If the generated input triggers new extreme values (e.g., variable value ranges, array access offsets, or stack sizes, etc.), its activation probability increases as follows:

$$P_m^{(t+1)} = P_m^{(t)} + \alpha, \quad (6)$$

while the probabilities for other mutations decrease proportionally:

$$P_i^{(t+1)} = P_i^{(t)} - \frac{\alpha}{l-1}, \quad i \neq m, \quad (7)$$

where α is a predefined update factor set at 0.04. These updates are subject to the following constraints:

$$\sum_{i=1}^l P_i^{(t+1)} = 1, \quad 0 \leq P_i^{(t+1)} \leq 1, \quad \forall i \in \{1, 2, \dots, l\}. \quad (8)$$

For example, in the second iteration (transitioning from $t=1$ to $t=2$), if mutation operation T_5 generated a test input that expanded the spectra extreme value, its activation probability increases from $P_5^{(1)} = 0.125$ to $P_5^{(2)} = P_5^{(1)} + \alpha = 0.125 + 0.04 = 0.165$, while the other operations adjust to $P_i^{(2)} = 0.119$ ($i \neq 3$).

An example illustrating the dynamic mutation guided by spectra feedback is shown in Table 2. The first column lists the test input IDs, while the second column displays the test inputs along with their corresponding mutation types T_m , where $m \in [1, 8]$, and $m \in \mathbb{Z}^+$, representing the eight designed mutation types. Columns 3 to 6 record the monitored variable types, names, and the current extreme values captured by the spectra monitoring script, whereas column 7 presents the corresponding real-time spectra ranges of the variables. The final column indicates the activation probability assigned to each mutation type. Initially, a test input seed [1, 1, 7, 5] is employed for HLS testing. In the first mutation round, each mutation type is assigned an activation probability of 0.125. Mutation type T_2 is activated, yielding a new test input (ID1: [1, 4, 2, 7]). Since the sizes and ranges of the variable spectra remain unchanged, the activation probabilities are maintained. Subsequently, mutation type T_5 is activated, producing a new test input (ID3: [1, 5, 8, 3]). At this point, the monitoring script detects that the variable *sum* attains a new extreme value of 17, prompting an increase in the activation probability for mutation type T_5 in subsequent mutations.

3.3.2 LLM-Guided Test Input Generation. Although dynamic mutation effectively minimizes ineffective mutations while ensuring broad coverage of the test input space, relying solely on mutation may not sufficiently explore the program's details. At this stage, by leveraging the semantic understanding and adaptive learning capabilities of LLMs, an LLM-guided test input generation mechanism is further proposed. Inspired by the Chain-of-Thought technique, an LLM-driven reasoning chain is employed to progressively analyze discrepancies between an HLS program and its corresponding

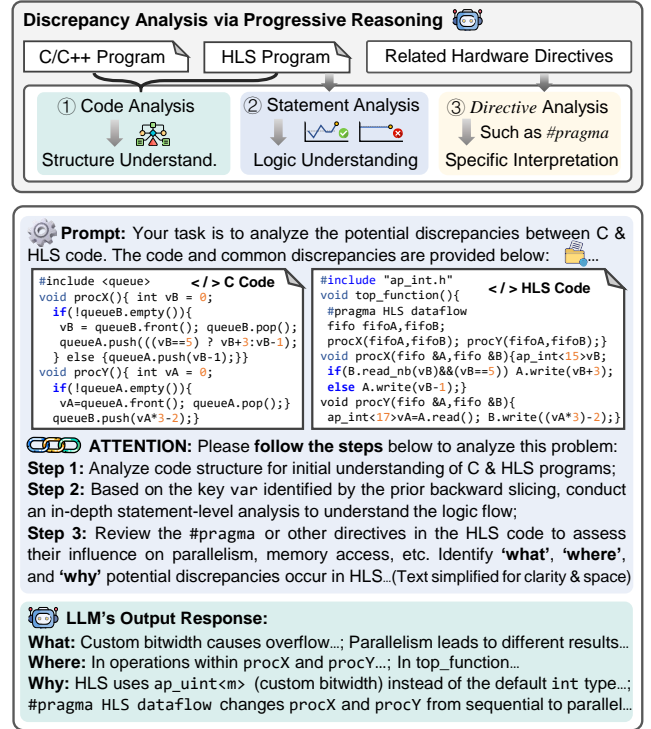


Figure 8: LLM-aided reasoning chain for progressive discrepancy analysis; (a) Execution steps; (b) Analysis example.

C/C++ program. As shown in Fig. 8, the process initiates with an overall code analysis to establish an understanding of the program structure. This is followed by a statement-level analysis that delves into the code logic by examining statements and function calls. Finally, a directive analysis phase focuses on hardware-specific interpretations, such as #typedef ap_int<n> and #pragma HLS pipeline, that can customize bit width or alter the execution mode. An example of the LLM-driven reasoning chain, including the associated prompts and responses, is provided at the bottom of Fig. 8, illustrating how the framework analyzes potential discrepancies for the test input generation. The key considerations for employing LLMs to generate test inputs for HLS programs are as follows:

(1) **HLS Program with Potential Discrepancies:** Building on the reasoning chain, the LLM systematically dissects potential discrepancies uncovered during overall code analysis, individual statement analysis, and directive analysis and then strategically designs targeted test inputs that hone in on these critical discrepancy points.

(2) **Task Scenario:** The application scenario, such as data encryption, image processing, or matrix computations, is embedded in the LLM prompts, enabling the LLM to generate test inputs that are aligned with the testing objectives.

(3) **Data Format Constraints:** HLS programs often have strict data format requirements. The customized data type specifies both the variable type and its bit width (e.g., ap_fixed<N> on FPGA), while the data structure defines the format of the input data, such as a one-dimensional array or a two-dimensional matrix, along with its dimensions (e.g., A[Row][Column] on FPGA). The prompts provided to the LLM need to clearly specify these format constraints to ensure that the generated test inputs meet the required specifications. In addition, the prompt should explicitly describe how

Table 3: Comparison of the proposed HLSTester with the GPT baseline and the traditional method.

Benchmark	Simulation Pass Rate of Generated Testbench for HLS (%)			Simulation Pass Rate of Instrumented Code for HLS (%)			Avg. Number of Detected Discrepancies (Same Time Budget)			Average Total Time Required to Test All Discrepancies (min)			
	Baseline	Proposed	Improve.	Baseline	Proposed	Improve.	Base.	Fuzz	Prop.	Baseline	Fuzz [16]	Proposed	Reduction
Greedy Algorithm	66.67	86.67	20	53.33	93.33	40	2	3	8	114.1	75.0	39.2	47.73%
Depth-First Search	80	93.33	13.33	73.33	86.67	13.33	2	2	6	209.2	157.8	113.8	27.88%
Advanced Encryption Standard	60	86.67	26.67	60	80	20	2	3	6	188.8	150.4	86.4	42.55%
K-Nearest Neighbor	86.67	100	13.33	73.33	86.67	13.33	1	3	7	209.2	174.4	72.9	58.20%
Gain Control	80	100	20	73.33	100	26.67	2	6	9	116.8	100.1	27.8	72.23%
Median Filter	66.67	93.33	26.67	60	93.33	33.33	2	2	9	177.5	147.2	99.6	32.34%
Deep Neural Network	73.33	86.67	13.33	53.33	80	26.67	1	2	8	206.5	169.8	56.6	66.67%
Edge Detection	53.33	80	26.67	60	86.67	26.67	2	4	8	211.9	192.0	100.2	47.81%
QR Decomposition	66.67	86.67	20	53.33	93.33	40	1	2	5	93.5	55.25	25.5	53.85%
Breadth-First Search	66.67	93.33	26.67	73.33	86.67	13.33	2	3	7	208.3	187.1	102.0	45.48%

* The simulation pass rate and testing performance metrics are calculated from the results of 15 rounds of HLS simulation.

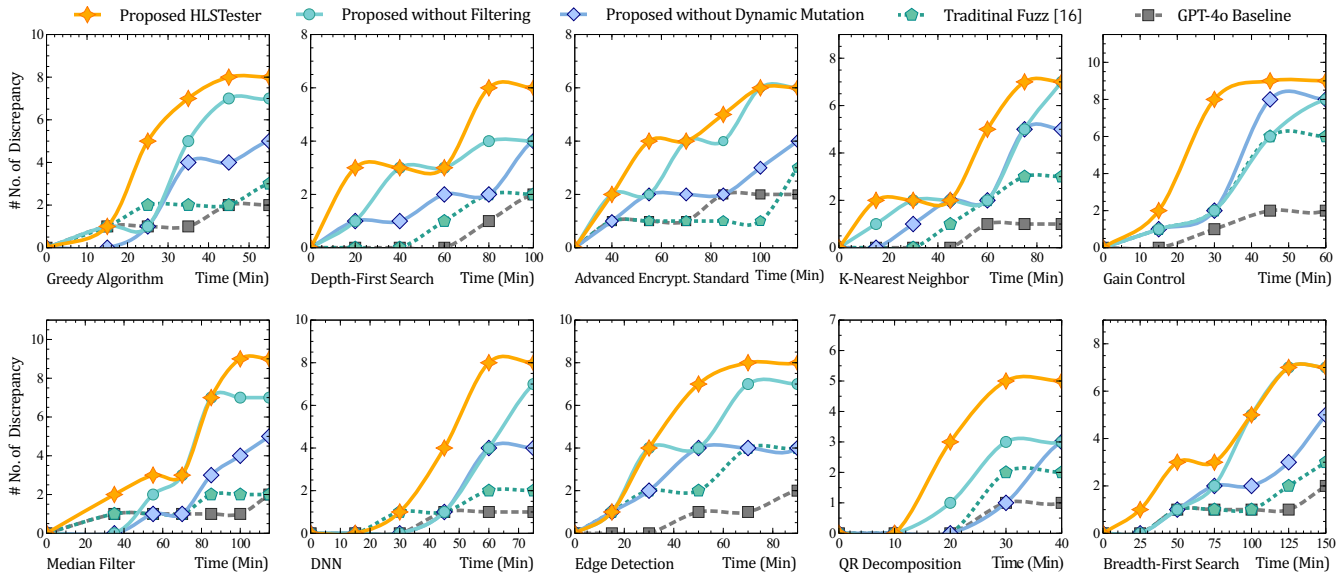


Figure 9: Comparison of the average number of behavioral discrepancies detected within the same time budget across ten real-world tasks, as shown on the x-axes of the figures.

the test inputs should be arranged. For example, generating one test input per line, separating values with spaces, and placing them between triple backticks. This ensures that the output format is correct and prevents testing failures due to formatting issues.

3.4 Redundancy-Aware Filtering of Test Inputs for Efficient Testing

To further reduce hardware testing latency, a redundancy-aware filtering mechanism is proposed to track the value ranges and data sizes of previously tested inputs, thereby avoiding re-simulation of inputs that are likely to exhibit the same behavioral discrepancies.

This mechanism dynamically maintains a global record table that stores the value ranges and data sizes of observed test inputs. When a new test input is generated, the framework first checks whether its value range or size exceeds those currently recorded. If the input’s range or size extends beyond the recorded range, it is likely to trigger new behaviors and hardware simulation will be executed. If the test input remains within the previously recorded range, it implies that the test input will not trigger new behavioral

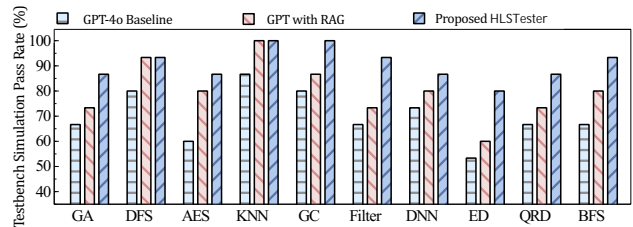


Figure 10: Comparison of the simulation pass rate of the generated HLS testbench among the proposed HLSTester, GPT baseline, and GPT with RAG.

discrepancies, and hardware simulation is skipped. For example, assume that the current recorded input range is (2, 5). If the input is [1, 4, 5], where the minimum value is lower than the recorded range, hardware simulation is executed, and the range is updated to (1, 5). However, if a subsequently generated input is [1, 3, 5], its range remains within (1, 5). Since inputs within the recorded range are likely to produce repetitive known discrepancies, the hardware simulation could be skipped, thereby enhancing testing efficiency by reducing unnecessary simulations.

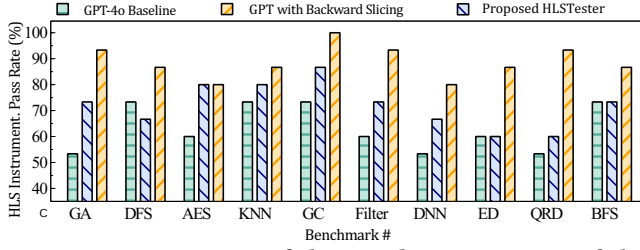


Figure 11: Comparison of the simulation pass rate of the instrumented HLS code among the proposed method, GPT baseline, and GPT with backward slicing.

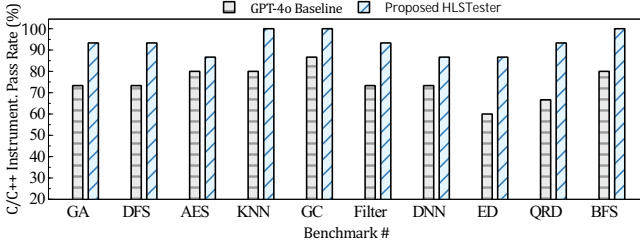


Figure 12: Comparison of the pass rate for instrumented C++ code between the proposed method and the GPT baseline.

4 EXPERIMENTAL RESULTS

We demonstrate the results of the proposed HLSTester across 10 real-world tasks in terms of the simulation pass rate of the generated testbench and instrumented program, the number of detected behavioral discrepancies within the same time budget, and the total time required for testing all behavioral discrepancies. Our benchmarks are from related work [36–38] covering different hardware directives (e.g., customized bit width, memory management, parallel operation, etc.), thereby exhibiting diverse behavior discrepancies.

During the evaluation, the GPT-4o model was employed as the LLM via OpenAI APIs [39]. All experiments were conducted using the Vitis HLS Tool to simulate program execution on a Xilinx Virtex UltraScale+ XCVU9P-FLGA2104I FPGA with an Intel(R) Xeon(R) Silver 4314 CPU. To ensure the reliability and statistical robustness of our evaluation, each experiment for a specific task was repeated n instances ($n = 15$). In each instance, the LLM was queried five times to iteratively correct the program based on the feedback from the HLS tool. We calculate the simulation pass rate as $\text{Pass Rate (\%)} = m/n$, where m represents the number of successfully generated instances and n denotes the total number of instances.

Table 3 compares the performance of the proposed HLSTester with the GPT baseline and the traditional testing method [15]. The first column lists the name of benchmark tasks, while the second through seventh columns show the simulation pass rates of the generated testbench and instrumented code for HLS, with the proposed framework demonstrating superior performance compared to the baseline. The eighth through tenth columns report the average number of detected behavioral discrepancies, demonstrating that the proposed HLSTester identifies more discrepancies within the same time budget. The final four columns detail the total time required to test all behavioral discrepancies and the corresponding reductions. According to these columns, the proposed HLSTester outperforms both the GPT baseline and the traditional method by achieving a higher pass rate and shorter overall testing time.

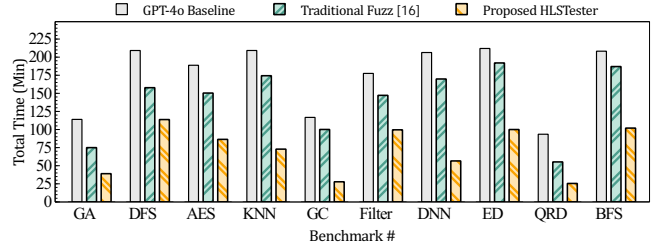


Figure 13: Comparison of the average total time required to test all behavioral discrepancies.

To demonstrate the effectiveness of the proposed method in testbench generation for HLS, we compare the simulation pass rate of the proposed HLSTester with using GPT directly. According to Fig. 10, the proposed HLSTester outperforms the baseline by achieving an average 20.67% increase in testbench generation.

Fig. 11 and Fig. 12 present comparisons of the simulation pass rate for code instrumentation, where the proposed framework was compared with the direct use of GPT and GPT with backward slicing. In these comparisons, the proposed LLM-aided framework demonstrated average improvements of 25.33% and 18.67% in HLS and C/C++ code instrumentation, respectively.

To demonstrate the acceleration achieved by the HLSTester in generating effective test inputs for efficient behavioral discrepancy detection, four baselines, including ablation options, were created by downgrading HLSTester in Fig. 9, which are summarized as follows:

- *GPT Baseline*: This baseline employs GPT directly to generate test inputs to detect behavioral discrepancies.
- *Traditional Fuzz Testing*: In this option, the HLS tool is invoked for every test input generated by fuzz testing.
- *Proposed without Mutation*: This option disables the proposed mutations from HLSTester.
- *Proposed without Redundancy-Aware Filtering*: In this option, redundancy filtering is disabled in HLSTester.

Fig. 9 compares the proposed HLSTester framework with four baselines in terms of behavioral discrepancy detection speed. The x-axis denotes the elapsed time (i.e., the testing time budget), while the y-axis shows the average cumulative number of detected discrepancies. Each data point represents the average of 15 repeated simulations per task. By incorporating an LLM-driven reasoning chain, dynamic mutation, and redundancy filtering, the proposed HLSTester generates more effective test inputs to detect more behavioral discrepancies in the same time budget. In particular, the LLM-driven reasoning chain achieves an average of $1.81\times$ speedup in detecting all behavioral discrepancies, while the dynamic mutation increases the speedup to an average of $2.28\times$, and the redundancy-aware technique further accelerates the testing workflow by 15.73%.

To evaluate the total testing time required to detect all behavioral discrepancies, Fig. 13 compares the proposed HLSTester with the direct use of GPT and traditional fuzz testing. Each bar represents the average total testing time per benchmark, which includes HLS tool compilation, synthesis and simulation time, GPT interaction time, script execution time, and so on. As illustrated, the proposed HLSTester achieves an average speedup of $2.71\times$ over the baseline, demonstrating the high efficiency achieved by optimizing the testing workflow.

5 CONCLUSION

In this paper, we propose HLSTester, an LLM-aided testing framework designed to efficiently detect behavioral discrepancies in HLS. Existing C/C++ testbenches are leveraged to guide the LLM in generating HLS-compatible testbenches that eliminate traditional C/C++ constructs incompatible with the HLS tool. Then, a backward slicing technique is employed to pinpoint the key variables, and a monitoring script is developed to record their runtime spectra, thereby enabling a detailed analysis of discrepancy symptoms. Moreover, a test input generation mechanism is proposed that leverages spectra feedback to guide dynamic mutation, which is incorporated with insights from an LLM-based progressive reasoning chain to increase the likelihood of revealing behavioral discrepancies. In addition, a redundancy-aware filtering technique is employed to skip repetitive simulations. Experimental results show that the proposed HLSTester significantly accelerates the testing workflow and achieves higher simulation pass rates compared with both the traditional method and the direct use of the LLM.

REFERENCES

- [1] Tinghuan Chen, Grace Li Zhang, Bei Yu, Bing Li, Ulf Schlichtmann, "Machine Learning in Advanced IC Design: A Methodological Survey," *IEEE Design & Test*, 2023.
- [2] Jason Cong, Bin Liu, Stephen Neundorffer, Juanjo Noguera, Kees Vissers, Zhiru Zhang, "High-Level Synthesis for FPGAs: From Prototyping to Deployment," *IEEE Transactions on Computer-Aided Design of Integrated Circuits and Systems*, 2011.
- [3] Jason Cong, Zhenman Fang, Muhuan Huang, Libo Wang, Di Wu, "CPU-FPGA Coscheduling for Big Data Applications," *IEEE Design & Test*, 2017.
- [4] Fan Cui, Youwei Xiao, Kexing Zhou, Yun Liang, "An Empirical Comparison of LLM-based Hardware Design and High-level Synthesis," *ACM International Symposium on Field-Programmable Gate Arrays (FPGA)*, 2025.
- [5] Qi Sun, Tinghuan Chen, Siting Liu, Jianli Chen, Hao Yu, Bei Yu, "Correlated Multi-objective Multi-fidelity Optimization for HLS Directives Design," *ACM Transactions on Design Automation of Electronic Systems (TODAES)*, 2022.
- [6] Licheng Guo, Pongstorn Maidee, Yun Zhou, Chris Lavin, Jie Wang, Yuze Chi, Weikang Qiao, Alireza Kaviani, Zhiru Zhang, Jason Cong, "RapidStream: Parallel Physical Implementation of FPGA HLS Designs," *ACM International Symposium on Field-Programmable Gate Arrays (FPGA)*, 2022.
- [7] Jason Lau, Aishwarya Sivaraman, Qian Zhang, Muhammad Ali Gulzar, Jason Cong, Miryung Kim, "Refactoring for Heterogeneous Computing with FPGA," *IEEE/ACM International Conference on Software Engineering (ICSE)*, 2020.
- [8] "Vitis High-Level Synthesis User Guide," Accessed: 2024. [Online]. Available: <https://docs.amd.com/r/2024.2-English/ug1399-vitis-hls/>.
- [9] Hao Zhou, Yang Liu, Hongji Wang, Enhao Tang, Shun Li, Yifan Zhang, Guohao Dai, Yongpan Liu, Kun Wang, "Deploying Diffusion Models with Scheduling Space Search and Memory Overflow Prevention Based on Graph Optimization," *IEEE/ACM Asia and South Pacific Design Automation Conference*, 2025.
- [10] Lena E. Olson, Jason Power, Mark D. Hill, and David A. Wood, "Border Control: Sandboxing Accelerators," *IEEE/ACM International Symposium on Microarchitecture (MICRO)*, 2015.
- [11] Lena E. Olson Mark D. Hill David A. Wood, "Crossing Guard: Mediating Host-Accelerator Coherence Interactions," *ACM Computer Architecture News*, 2017.
- [12] Jianyi Cheng, Lianghui Wang, Zijian Jiang, Yungang Bao, Kan Shi, "Latency Insensitivity Testing for Dataflow HLS Designs," *ACM International Symposium on Field-Programmable Gate Arrays (FPGA)*, 2025.
- [13] Parmida Vahdatniya, Amirali Sharifian, Reza Hojabr, Arrvinth Shriraman, "Mugrind: A Framework for Dynamically Instrumenting HLS-Generated RTL," *ACM International Conference on Parallel Architectures*, 2022.
- [14] Jianyi Cheng, Lianghui Wang, Zijian Jiang, Yungang Bao, Kan Shi, "Latency Insensitivity Testing for Dataflow HLS Designs," *ACM International Symposium on Field-Programmable Gate Arrays (FPGA)*, 2025.
- [15] Michal Zalewski, "American Fuzzy Lop (AFL)," Accessed: 2024. [Online]. Available: <https://lcamtuf.coredump.cx/afl/>.
- [16] Valentin Manes, HyungSeok Han, Choongwoo Han, sang cha, Manuel Egele, Edward Schwartz, Maverick Woo, "The Art, Science, and Engineering of Fuzzing: A Survey," *IEEE Transactions on Software Engineering*, 2019.
- [17] Michael Pellauer, Michael Adler, Michel Kinsky, Angshuman Parashar, Joel Emer, "HAsim: FPGA-based high-detail multicore simulation using time-division multiplexing," *IEEE/ACM International Symposium on High Performance Computer Architecture (HPCA)*, 2011.
- [18] Johannes Menzel, Christian Plessl, Tobias Kenter, "The Strong Scaling Advantage of FPGAs in HPC for N-body Simulations," *ACM Transactions on Reconfigurable Technology and Systems (TRETS)*, 2021.
- [19] Chenwei Xiong, Cheng Liu, Huawei Li, Xiaowei Li, "HLSPIlot: LLM-based High-Level Synthesis," *IEEE International Conference on Computer-Aided Design*, 2024.
- [20] Yingbing Huang, Lily Jiabin Wan, Hanchen Ye, Manvi Jha, Jinghua Wang, Yuhong Li, Xiaofan Zhang, Deming Chen, "New solutions on LLM acceleration, optimization, and application," *IEEE/ACM Design Automation Conference (DAC)*, 2024.
- [21] Mingjie Liu, Nathaniel Pinckney, Bruce Khailany, Haoxing Ren, "VerilogEval: Evaluating large language models for verilog code generation," *IEEE/ACM International Conference on Computer Aided Design (ICCAD)*, 2023.
- [22] Kaiyan Chang, Kun Wang, Nan Yang, Ying Wang, Yinhe Han, Huawei Li, Xiaowei Li, "Data is all you need: Finetuning LLMs for Chip Design via an Automated design-data augmentation framework," *IEEE Design Automation Conference*, 2024.
- [23] Kangwei Xu, Ruidi Qiu, Zhuorui Zhao, Grace Li Zhang, Ulf Schlichtmann, Bing Li, "LLM-Aided Efficient Hardware Design Automation," *arXiv: 2410.18582*, 2024.
- [24] Jingcun Wang, Yu-Guang Chen, Ing-Chao Lin, Bing Li, Grace Li Zhang, "Basis Sharing: Cross-Layer Parameter Sharing for Large Language Model Compression," *International Conference on Learning Representations (ICLR)*, 2025.
- [25] Ruidi Qiu, Grace Li Zhang, Rolf Drechsler, Ulf Schlichtmann, Bing Li, "AutoBench: Automatic Testbench Generation and Evaluation Using LLMs for HDL Design," *ACM/IEEE International Symposium on Machine Learning for Computer-Aided Design (MLCAD)*, 2024.
- [26] Zhuorui Zhao, Ruidi Qiu, Ing-Chao Lin, Grace Li Zhang, Bing Li, Ulf Schlichtmann, "VRank: Enhancing Verilog Code Generation from Large Language Models via Self-Consistency," *ACM/IEEE International Symposium on Quality Electronic Design (ISQED)*, 2025.
- [27] Wenhao Sun, Bing Li, Grace Li Zhang, Xunzhao Yin, Cheng Zhuo, Ulf Schlichtmann, "Paradigm-Based Automatic HDL Code Generation Using LLMs," *ACM/IEEE International Symposium on Quality Electronic Design (ISQED)*, 2025.
- [28] Yuwei Zhang, Qingyuan Lu, Kai Liu, Wensheng Dou, Jiabin Zhu, Li Qian, Chunxi Zhang, Zheng Lin, Jun Wei, "CITYWALK: Enhancing LLM-Based C++ Unit Test Generation via Project-Dependency Awareness and Language-Specific Knowledge," *arXiv preprint: 2501.16155*, 2025.
- [29] Ruidi Qiu, Grace Li Zhang, Rolf Drechsler, Ulf Schlichtmann, Bing Li, "CorrectBench: Automatic Testbench Generation with Functional Self-Correction using LLMs for HDL Design," *IEEE/ACM Design, Automation & Test in Europe Conference & Exhibition (DATE)*, 2025.
- [30] Ruiyang Ma, Yuxin Yang, Ziqian Liu, Jiayi Zhang, Min Li, Junhua Huang, Guojie Luo, "VerilogReader: LLM-Aided Hardware Test Generation," *IEEE International Workshop on LLM-Aided Design (LAD)*, 2024.
- [31] Qian Zhang, Jiyuan Wang, Guoqing Harry Xu, Miryung Kim, "HeteroGen: transpiling C to heterogeneous HLS code with automated test generation and program repair," *ACM International Conference on Architectural Support for Programming Languages and Operating Systems (ASPLOS)*, 2022.
- [32] Johannes de Fine Licht, Maciej Besta, Simon Meierhans, Torsten Hoefler, "HTransformations of High-Level Synthesis Codes for High-Performance Computing," *IEEE Transactions on Parallel and Distributed Systems (TPDS)*, 2021.
- [33] David B. Thomas, "Synthesizable recursion for C++ HLS tools," *IEEE International Conference on Application-Specific Systems, Architectures and Processors*, 2016.
- [34] Yann Herklotz and John Wickerson, "Finding and Understanding Bugs in FPGA Synthesis Tools," *IEEE/ACM International Symposium on Field-Programmable Gate Arrays (FPGA)*, 2020.
- [35] Kevin Lauerer, Jack Koenig, Donggyu Kim, Jonathan Bachrach and Koushik Sen, "RFUZZ: Coverage-Directed Fuzz Testing of RTL on FPGAs," *IEEE/ACM International Conference on Computer-Aided Design (ICCAD)*, 2018.
- [36] Kangwei Xu, Grace Li Zhang, Xunzhao Yin, Cheng Zhuo, Ulf Schlichtmann, Bing Li, "Automated C/C++ Program Repair for High-Level Synthesis via Large Language Models," *IEEE/ACM International Symposium on Machine Learning for CAD (MLCAD)*, 2024.
- [37] "Open Source Computer Vision (OpenCV)," Accessed: 2024. [Online]. Available: <https://docs.opencv.org/>.
- [38] "LeetCode Problem Set," Accessed: 2023. [Online]. Available: <https://leetcode.com/problemset/>.
- [39] "GPT through OpenAI API," Accessed: 2024. [Online]. Available: <https://platform.openai.com/>.
- [40] W. Eric Wong, Ruizhi Gao, Yihao Li, Rui Abreu, Franz Wotawa, "A Survey on Software Fault Localization," *IEEE Transactions on Software Engineering*, 2016.
- [41] James Kukucka, Luis Pina, Paul Ammann, and Jonathan Bell, "An Empirical Examination of Fuzzer Mutator Performance," *ACM International Symposium on Software Testing and Analysis (ISSTA)*, 2024.
- [42] Patrick Jauernig, Domagoj Jakobovic, Stjepan Picek, Emmanuel Stempf, Ahmad-Reza Sadeghi, "DARWIN: Survival of the Fittest Fuzzing Mutators," *Network and Distributed System Security Symposium*, 2023.
- [43] Nils Reimers, Iryna Gurevych, "Sentence-BERT: Sentence Embeddings using Siamese BERT-Networks," *ACL Empirical Methods in Natural Language Processing (EMNLP)*, 2019.